

# INFLUENCE OF RESIDUAL STRESSES ON THE CRACK DRIVING FORCE IN BIMATERIALS WITH SHARP INTERFACE

M. Rakin<sup>1,2\*</sup>, O. Kolednik<sup>1</sup>, N.K. Simha<sup>3</sup> and F.D. Fischer<sup>1,4</sup>

<sup>1</sup> Erich Schmid Institute of Materials Science, Austrian Academy of Sciences, A-8700 Leoben, Austria

<sup>2</sup> Materials Center Leoben, A-8700 Leoben, Austria

<sup>3</sup> University of Miami, Coral Gables, FL 33124-0642, USA

<sup>4</sup> Institute of Mechanics, Montanuniversität Leoben, A-8700 Leoben, Austria

## ABSTRACT

The paper considers the effect of residual stresses in pre-cracked bimaterial fracture mechanics specimens with a sharp interface. The residual stresses produce a shielding or anti-shielding effect on the crack tip by inducing an additional crack driving force term, the material inhomogeneity term,  $C_{inh}$ . The residual stresses are introduced by a cooling of the specimen from an elevated temperature to the room temperature. Subsequently, the specimen is statically loaded. The material inhomogeneity term,  $C_{inh}$ , is evaluated by a post-processing procedure, following a conventional finite element stress analysis. The values of the J-integrals around the crack tip,  $J_{tip}$ , and around the external boundaries,  $J_{far}$ , are also computed. During the loading sequence, additionally, the experimental J-integral,  $J_0$ , is evaluated, which is determined according to the standard procedures from the area below the load vs. load line displacement curve. As a first example, an elastic-ideally plastic bimaterial is considered with different coefficients of thermal expansion, but otherwise homogeneous mechanical properties.

## 1 INTRODUCTION

Residual stresses are inherent to many inhomogeneous materials or structural components, mostly produced during the fabrication due to the cooling from an elevated temperature. The residual stresses produce a shielding or anti-shielding effect on the crack tip and, thus, the crack driving force becomes different, compared to a homogeneous material without residual stresses, see [1-4]. The quantitative description of this effect is essential for the understanding of the behavior of inhomogeneous materials or components during monotonic or cyclic loading.

It is known long since that inhomogeneous material properties can affect the effective crack driving force, see [5,6] for a literature review. In recent papers, the concept of material forces, [6,7], has been used to investigate the inhomogeneity effect. It has been shown [8,9] that material inhomogeneities in the direction of the crack extension induce an additional crack driving force term, called the material inhomogeneity term,  $C_{inh}$ . The effective crack driving force, stated in terms of the J-integral around the crack tip,  $J_{tip}$ , is given by the sum of the far-field J-integral,  $J_{far}$ , and the material inhomogeneity term,

$$J_{tip} = J_{far} + C_{inh} . \quad (1)$$

The magnitude of the material inhomogeneity term,  $C_{inh}$ , can be evaluated by a post-processing procedure, following a conventional numerical stress analysis. In preceding investigations, the effect of material inhomogeneities has been explored for linear elastic or elastic-plastic bimaterial specimens with sharp and graded interfaces. A mismatch in the elastic modulus, the yield stress, or the strain hardening exponent at the interface has been considered, as

---

\* on leave from the Faculty of Technology and Metallurgy, University of Belgrade, Belgrade, Serbia and Montenegro.

well as the effects of mismatch combinations [8-11]. It has been found that the material inhomogeneity term,  $C_{inh}$ , is positive and the effective crack driving force,  $J_{tip}$ , becomes larger than the far-field J-integral,  $J_{far}$ , if a crack grows towards a more compliant and/or lower strength material. A transition into a stiffer and/or higher strength material leads to a negative  $C_{inh}$ , and  $J_{tip}$  becomes smaller than  $J_{far}$ .

The effects of residual stresses, however, have been neglected so far. This is the reason why these effects are the subject of this paper.

## 2 NUMERICAL MODELING

We consider a standard compact tension bimaterial specimen made of two homogeneous materials which are perfectly bonded along a sharp interface. The specimen dimensions are: width  $W=50$  mm, thickness  $B=25$  mm, initial crack length  $a_0=29$  mm, distance between crack tip and interface  $L=2.5$  mm. To explore only the effect of thermal residual stresses, the two materials are assumed to have a different coefficient of thermal expansion (CTE),  $12 \times 10^{-6}$  and  $17 \times 10^{-6} \text{ K}^{-1}$ , as for ferritic and austenitic steels. Otherwise, the materials shall have homogeneous, isotropic mechanical properties with a Young's modulus,  $E=210$  GPa, a Poisson's ratio,  $\nu=0.3$ , and a yield stress,  $\sigma_y=500$  MPa, without strain hardening. In the following, we denote the material with the higher CTE as ‘‘austenitic steel’’, the material with the lower CTE as ‘‘ferritic steel’’.

The residual stresses are introduced by ‘‘cooling’’ the specimen from different elevated temperatures to the room temperature. Heat transfer is not considered. Thus, the introduced temperature intervals are used only to cause residual stress fields, in a quasi-static analysis. After the cooling, the specimen is loaded by prescribing the load line displacement.

The material inhomogeneity term,  $C_{inh}$ , has been derived from the concept of material forces for a continuous variation of the material properties [8] and for discrete jumps of the material properties along interfaces [9]. The equations for a combined effect of both smooth variations and interfaces are given in [12]. Moreover, in that paper the influences of eigenstrains, thermal strains, and residual stresses are treated. It is shown that in the linear setting the material inhomogeneity term can be written as

$$C_{inh} = -e_j \int_D \frac{\partial \phi(\boldsymbol{\varepsilon}_{pq}, x_p)}{\partial x_j} dA - \sum_{i=1}^k \int_{\Sigma^i} \left( [[\phi]] - \langle \sigma_{pq} \rangle [[\varepsilon_{pq}]] \right) (n_j^i e_j) ds. \quad (2)$$

In Eqn (2),  $\phi$  is the stored energy density which depends on the linear strain,  $\boldsymbol{\varepsilon}$ , and has an explicit dependence on the reference coordinate,  $\mathbf{x}$ . The region  $D$  denotes the area between the two contours which are used to evaluate the near-tip and far-field J-integrals, and it is assumed that there are  $i=1,2,\dots,k$  sharp interfaces,  $\Sigma^i$ , within the region  $D$ . The symbol  $[[\phi]]$  denotes the jump of the strain energy density and  $[[\varepsilon_{ik}]]$  the jump of the strain components at an interface;  $\langle \sigma_{ik} \rangle$  denotes the mean value of the local stress components on both sides of the interface. Finally,  $n_j$  is the unit normal vector to the interface and  $e_j$  is the unit vector in the direction of the crack growth. It should be noted that in case of  $k$  interfaces within the region  $D$ , the integration of the first term in Eqn (2) is performed in  $(k+1)$  subregions formed between the interfaces.

If the materials left and right of the interfaces are homogeneous, the area integral in Eqn (2) does not contribute, and for a jump of the material properties at a single interface,  $\Sigma$ , Eqn (2) reduces to

$$C_{inh} = - \int_{\Sigma} \left( [[\phi]] - \langle \sigma_{pq} \rangle [[\varepsilon_{pq}]] \right) (n_j e_j) ds. \quad (3)$$

After a finite element stress analysis, the material inhomogeneity term,  $C_{inh}$ , can be evaluated by a simple post processing procedure [9,10]. The stress analysis is performed, using a finite element program (ABAQUS, Vers. 6.2, www.hks.com). The mesh for the two-dimensional plane strain analysis with a stationary crack consists of isoparametric 8-node elements; at the crack tip singular elements are used. More details are given in [10].

During the loading sequence of the specimen, the experimental J-integral,  $J_0$ , is evaluated from the area,  $U$ , below the load vs. load line displacement curve, as determined in a fracture mechanics experiment according to the ESIS procedure [13],

$$J_0 = \frac{\eta U}{b_0 B} \quad (4)$$

In Eqn (4),  $\eta$  is a geometry factor which is close to 2.2, and  $b_0 = W - a_0$  is the ligament length.

### 3 RESULTS

In Figure 1, the influence of the cooling temperature interval,  $-\Delta T$ , on the material inhomogeneity term,  $C_{inh}$ , and the near-tip and far-field J-integrals,  $J_{tip}$  and  $J_{far}$ , is shown for a bimaterial specimen with the crack situated in the austenitic steel. For small temperature intervals (less than 150°C), the  $C_{inh}$ - and  $J_{far}$ - curves have a parabolic shape, corresponding to an elastic straining of the materials. For higher temperature intervals, the materials start to deform plastically and the curves become linear. The effective crack driving force,  $J_{tip}$ , is positive and small. This is in correspondence to a small, positive value of the crack tip opening displacement, CTOD. As  $J_{tip}$  is so small, of the order of 1 kJ/m<sup>2</sup>, and Eqn (1) is fulfilled very accurately,  $J_{far}$  and  $C_{inh}$  have almost the same absolute magnitude. The opposite arrangement of the materials in the bimaterial specimen (crack in the ferritic steel) leads to  $J_{tip}$ -,  $J_{far}$ -, and  $C_{inh}$ -values of nearly the same magnitude but the opposite sign. Figure 2 presents the development of  $C_{inh}$ ,  $J_{tip}$ , and  $J_{far}$  during the loading of the specimen. The parameters are plotted against the load-line displacement,  $v_{LL}$ . Additionally, the values of the experimental J-integral,  $J_0$ , are shown. It should be noted that due to the thermal strains, the curves do not start from  $v_{LL} = 0$ . (Imagine a specimen which is machined after the cooling from a larger

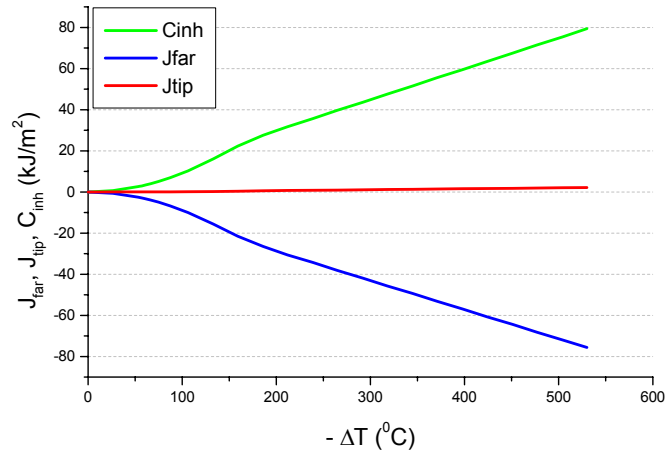


Figure 1: Effect of the temperature interval during the cooling on the material inhomogeneity term,  $C_{inh}$ , and the near-tip and far-field J-integrals,  $J_{tip}$  and  $J_{far}$ , for a bimaterial specimen with an inhomogeneity of the CTE.

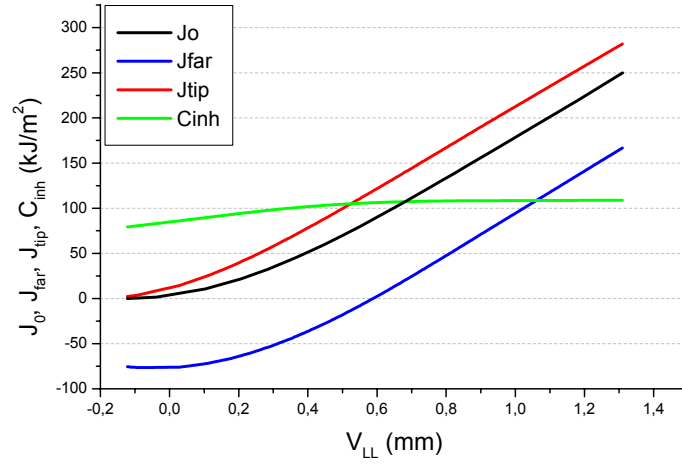


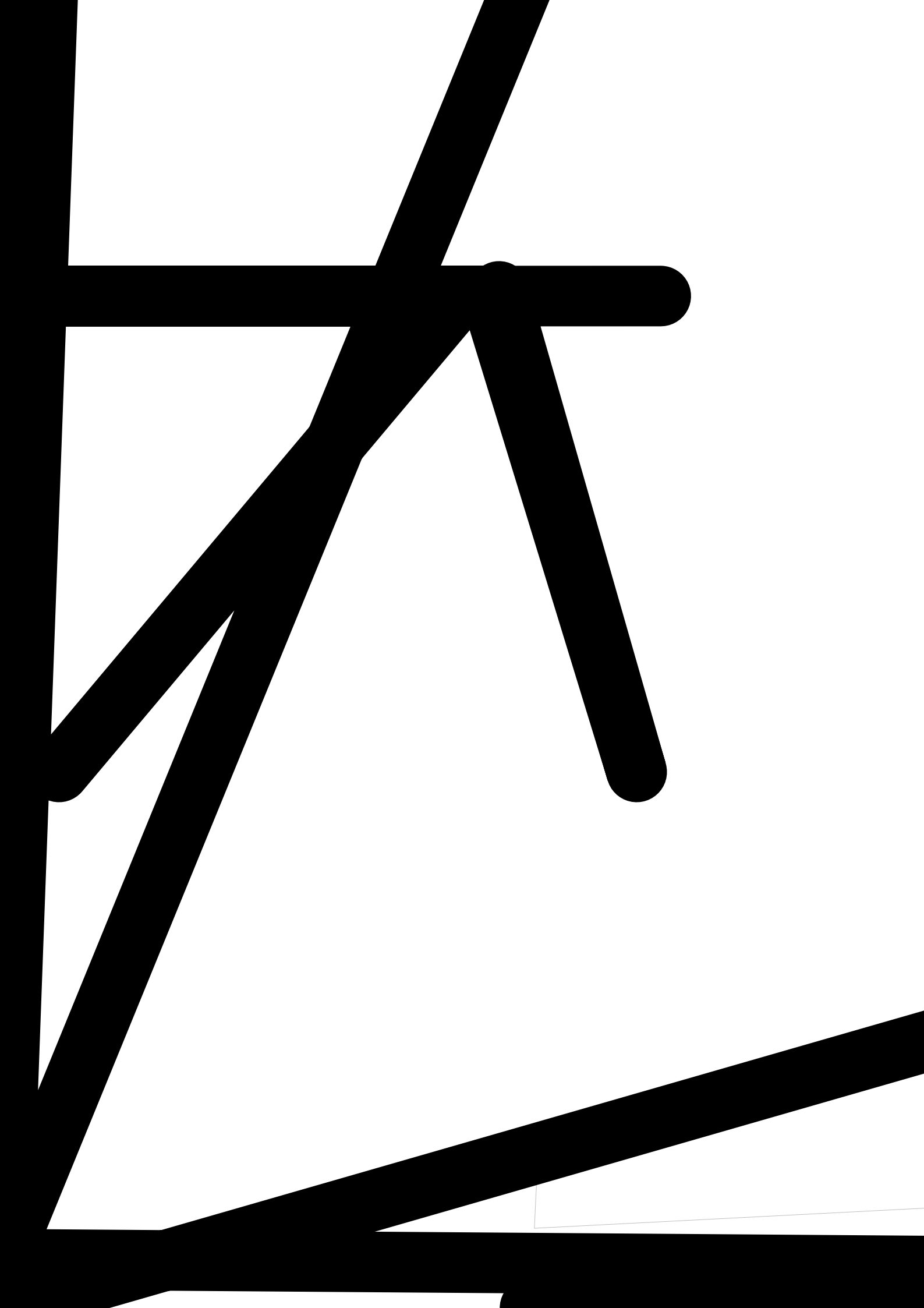
Figure 2: Effect of the loading on the parameters  $C_{inh}$ ,  $J_{tip}$ ,  $J_{far}$ , and the experimental J-integral,  $J_0$ , for a bimaterial specimen with an inhomogeneity of the CTE.

bimaterial block. Then, the same curves would appear, but shifted parallel so that they start at  $v_{LL} = 0$ .) The material inhomogeneity term,  $C_{inh}$ , increases only slightly and remains then constant, as the materials left and right of the interface have the same mechanical properties. The parameters  $J_{tip}$ ,  $J_{far}$ , and  $J_0$  increase first parabolically and then linearly with increasing  $v_{LL}$ . The effective crack driving force,  $J_{tip}$ , is always larger than  $J_0$ ; the difference is, e.g., 35.5% at  $v_{LL} = 0.6$  mm. The differences between  $J_{far}$  and  $J_0$  are even more significant. For the opposite arrangement of the materials in the bimaterial specimen (crack in the ferritic steel),  $J_{tip}$  is about 18% smaller than  $J_0$  at  $v_{LL} = 0.6$  mm

#### 4 DISCUSSION

In previous investigations [9,10], the effect of material inhomogeneities on the effective crack driving force was investigated for similar bimaterial specimens. In these investigations, it was assumed that the specimens are free of residual stresses. Figure 3 presents the results for a bimaterial specimens consisting of two elastic-ideally plastic materials which have the same yield stress,  $\sigma_y = 500$  MPa, but different Young's modulus,  $E = 210$  and  $70$  GPa, respectively. The distance between crack tip and interface is  $L = 1.25$  mm. As the crack is in the material with the higher Young's modulus, the material inhomogeneity term is positive and the effective crack driving force,  $J_{tip}$ , is larger than  $J_{far}$ . In these investigations,  $J_{far}$  was termed as "nominally applied crack driving force" and it was implicitly assumed that  $J_{far}$  coincides with the experimental J-integral,  $J_0$ . It is seen from Figure 3 that this assumption was correct, as the  $J_{far}$ - and  $J_0$ -curves nearly coincide. The small difference might be caused by an inaccuracy of the geometry factor  $\eta$  in Eqn (4), or by numerical inaccuracies. It has been demonstrated in Figures 1 and 2 that the above assumption is not valid and  $J_{far}$  and  $J_0$  can differ strongly, when residual stresses appear in the specimen.

The direct computation of  $J_{tip}$  using the virtual crack extension method of ABAQUS might include some inaccuracy, especially, if the distance between crack tip and interface becomes small, and it is more accurate to evaluate the effective crack driving force via Eqn (1) from the values of  $J_{far}$  and  $C_{inh}$ , which are determined more accurately. In the cases presented here, however, the curves of  $J_{tip}$  and  $(J_{far} + C_{inh})$  nearly coincide.



#### ACKNOWLEDGEMENTS

The authors acknowledge gratefully the Materials Center Leoben for funding this work under the project number SP14.

#### REFERENCES

1. Shih C.F., Moran B., Nakamura T., Energy release rate along three-dimensional crack front in a thermally stressed body, *International Journal of Fracture*, Vol 30, 79-102, 1986.
2. Hou Y.C., Pan J., A fracture parameter for welded structures with residual stresses, *Computational Mechanics*, Vol. 22, 281-288, 1998.
3. Meith W.A., Hill M.R., Domain-independent values of the J-integral for cracks in three-dimensional residual stress bearing bodies, *Engineering Fracture Mechanics*, Vol 69, 1301-1314, 2002.
4. Lei Y., O'Dowd N.P., Webster G.A., J estimation and defect assessment for combined residual stress and mechanical loading, *International Journal of Pressure Vessels and Piping*, Vol. 77, 321-333, 2000.
5. Kolednik, O., The yield-stress gradient effect in inhomogeneous materials, *International Journal of Solids and Structures*, Vol. 37, 781-808, 2000.
6. Maugin, G.A., *Material Inhomogeneities in Elasticity*, Chapman and Hall, London, 1993.
7. Gurtin, M.E., *Configurational Forces as Basic Concepts of Continuum Physics*, Springer, Berlin, 2000.
8. Simha, N.K., Fischer, F. D., Kolednik, O., Chen, C. R., Inhomogeneity effects on the crack driving force in elastic and elastic-plastic materials, *Journal of the Mechanics and Physics of Solids*, Vol. 51, 209-240, 2003.
9. Simha, N.K., Predan, J., Kolednik, O., Shan, G.X., Fischer, F. D., Inhomogeneity effects on the crack driving force in elastic and elastic-plastic materials. Part II: Sharp interfaces, *Journal of the Mechanics and Physics of Solids*, submitted.
10. Kolednik, O., Predan, J., Shan, G.X., Simha, N.K., Fischer, F. D., On the fracture behavior of inhomogeneous materials – a case study for elastically inhomogeneous bimetals, *International Journal of Solids and Structures*, in press, 2004.
11. Kolednik, O., Predan, J., Shan, G.X., Simha, N.K., Fischer F.D., Crack-tip shielding and anti-shielding by a bimaterial interface, in *Proceedings of the 15<sup>th</sup> European Conference of Fracture*, submitted.
12. N.K. Simha, O. Kolednik, F.D. Fischer, Material force models for cracks – influences of eigenstrains, thermal strains & residual stresses, in *Proceedings of the 11<sup>th</sup> International Conference on Fracture*, submitted
13. ESIS Procedure for determining the fracture behaviour of materials, European Structural Integrity Society, ESIS P2-92, 1992.